jESE

Original scientific paper

Copper-nickel oxide nanofilm modified electrode for non-enzymatic determination of glucose

Mahsa Hasanzadeh[1,✉], Zahra Hasanzadeh[1], Sakineh Alizadeh[2], Mehran Sayadi[3,✉], Mojtaba Nasiri Nezhad[4], Reza E. Sabzi[1] and Sajjad Ahmadi[1]

[1]Department of Analytical Chemistry, Faculty of Chemistry, University of Urmia, Urmia, Iran
[2]Faculty of Chemistry, Bu-Ali Sina University, Hamadan, Iran
[3]Department of Food Safety and Hygiene, School of Health, Fasa University of Medical Science, Fasa, Iran
[4]Department of Chemical Engineering, Urmia University of Technology, Urmia, Iran

Corresponding authors: ✉ mahsa.hasanzadeh95@gmail.com; ✉tmf_fmt3000@yahoo.com

Abstract

Cu_xO-NiO nanocomposite film for the non-enzymatic determination of glucose was prepared by the novel modifying method. At first, anodized Cu electrode was kept in a mixture solution of $CuSO_4$, $NiSO_4$ and H_2SO_4 for 15 minutes. Then, a cathodization process with a step potential of -6 V in a mixture solution of $CuSO_4$ and $NiSO_4$ was initiated, generating formation of porous Cu-Ni film on the bare Cu electrode by electrodeposition assisted by the release of hydrogen bubbles acting as soft templates. Optimized conditions were determined by the experimental design software for electrodeposition process. Afterward, Cu-Ni modified electrode was scanned by cyclic voltammetry (CV) method in NaOH solution to convert Cu and Ni nanoparticles to the nano-scaled Cu_xO-NiO film. The electrocatalytic behavior of the novel Cu_xO-NiO film toward glucose oxidation was studied by CV and chronoamperometry (CHA) techniques. The calibration curve of glucose was found linear in a wide range of 0.04–5.76 mM, with a low limit of detection (LOD) of 7.3 µM (S/N = 3) and high sensitivity (1.38 mA mM^{-1} cm^{-2}). The sensor showed high selectivity against some usual interfering species and high stability (loss of only 6.3 % of its performance over one month). The prepared Cu_xO-NiO nanofilm based sensor was successfully applied for monitoring glucose in human blood serum and urine samples.

Keywords

CuxO; NiO; nanofilm; Cu electrode; modifying method; non-enzymatic glucose sensor.

Introduction

In electro-biochemical analysis, it is generally believed that sensing interfaces play key roles in the enzyme-less detection of biomolecules like glucose, ascorbic acid (AA), dopamine (DA) and uric acid

(UA) [1]. Glucose detection is essential in clinical diagnosis, biotechnology and food industry [2]. Over past decades, a number of studies was performed on alleviating drawbacks of enzymatic glucose sensors [3]. The majority of known amperometric biosensors for glucose monitoring use glucose oxidase (GOD) or glucose dehydrogenase enzymes [4,5]. The most common and serious problem is insufficient stability resulted from the nature of the enzymes which could hardly be restrained. Although GOD is quite stable compared to other enzymes, glucose sensors based on GOD are always exposed to a possibility of thermal and chemical deformation during fabrication, storage or use. Furthermore, GOD quickly loses its activity below pH 2 and above pH 8, and also, temperatures above 40 °C can cause fatal damages [3]. Ionic detergents also deactivate GOD. At the other side, glucose dehydrogenase enzyme showed the problem of effectiveness from interfering species like AA, DA, *etc.* [6,7], unless a selective membrane for reducing effect of interfering species was used [8]. To overcome the above obstacles, non-enzymatic glucose sensors are developed coming closer to practical applications [6]. Non-enzymatic glucose sensors have received significant interest due to their advantage of thermal and chemical stability [7]. In order to prepare a non-enzymatic glucose sensor, nanostructured particles have attracted extensive scientific and industrial interests due to their unique electronic, optical and catalytic properties [9]. Moreover, when utilizing nanomaterials, it becomes possible to minimize the influence of interfering substances such as AA and UA [10]. Various nanostructured materials have been proposed as new opportunities to develop novel non-enzymatic glucose sensors [6] such as carbon nanotubes [11], metals [12,13], metal oxides such as NiO [14-17] or Cu_2O [18], metal composites such as Cu-Ni [19], *etc.* Different methods were already reported for preparations of different forms of Cu-Ni film for determining various materials, such as preparation of Cu-Ni alloys used in electrochemical oxygen analysis [20] or preparation of Cu and Ni nanoparticles deposited on ITO electrode for non-enzymatic electrochemical carbohydrates sensor applications [21]. In addition, Cu@Ni/MWCNT nanocomposite was prepared for simultaneous electrochemical determination of guanine and adenine [22], Cu@Ni core–shell nanoparticles/reduced graphene oxide nanocomposite for non-enzymatic glucose sensor [23], and non-enzymatic multispecies sensor based on Cu-Ni nanoparticle dispersion on doped graphene [19].

The goal of this work is preparation of the novel Cu-Ni nanofilm on an inexpensive electrode like Cu, which should serve as fast, low-cost and easy method for the non-enzymatic glucose determination. A novel procedure of Cu_xO-NiO nanocomposite fabrication is proposed, involving hydrogen bubbles evolution serving as soft templates for electrodeposition of porous Cu-Ni nanofilm. Finding of optimized conditions for electrodeposition is based on a famous statistical method called the response surface methodology (RSM). RSM method is widely applicable in electrochemistry and other research fields for gaining some important information for optimizing experimental conditions by considering the interactions between model factors instead individual variables. Deposition potential, time of deposition and volume combination of Ni-Cu solutions are chosen as model factors in electrodeposition. The prepared novel nanocomposite Cu_xO-NiO film is studied by CV and CHA techniques and tested for amperometric determination of glucose in practical samples of human blood serum and urine.

Experimental

Reagents and chemicals

CuSO₄×5H₂O, NiSO₄×6H₂O, NaOH, AA, UA, DA and H₂SO₄ were all purchased from Merck Co. Blood serum samples were obtained from a local hospital. For glucose determination, 0.1 M NaOH

solution was used as the electrolyte. Double distilled (DD) water was applied in preparing all solutions.

Apparatus and electrochemical measurements

Electrochemical experiments were performed in a three-electrode cell, µAutolab type III (Netherlands). Agilent technologies DC power supply N5752A (USA) was used for applying -6 V potential. Cu rod electrode (3 mm in diameter), Ag/AgCl (KCl saturated) electrode and a piece of Pt wire were used as working, reference and counter electrode, respectively. Ultrasonicator (Pars Nahad Co., Iran) was applied to clean the electrode surface from impurities. Field emission scanning electron microscopy (FESEM) images were obtained by a MIRA3 TESCAN SEM system [Razi Metallurgical Research Center (RMRC), Iran]. X-ray diffraction (XRD) measurements were done at Urmia University. Optimized conditions were determined by the experimental design. All calculations and programming for the experimental design were performed in MATLAB (Hyper-cube Inc. Version10) software. The essential regression and experimental design for chemists and engineers (Eregress) excel were added in software. All experiments were conducted in stationary solutions except tests relevant to a hydrodynamic CHA method, which were conducted using a magnetic stirrer with a constant rotation speed of 150 rpm. All parameters affecting the experiments including concentrations of solutions, volume ratios of solutions, electrolyte concentrations, applied step potential and its duration time, were optimized. All experiments were performed at room temperature (25 °C) and repeated at least three times.

Modified electrode fabrication

Bare Cu electrode was firstly polished with 400 and 2000 grit emery papers respectively, and washed to remove impurities. Then, the electrode was immersed into DD water and ultrasonicated for few minutes. Afterwards, the surface of the electrode was washed with DD water again to clean any surface impurity. After polishing and cleaning of the surface, the electrode was anodized electrochemically by CHA method with an applied potential of +1.5 V for 40 s in 0.1 M NaOH. Then, the electrode was washed carefully with DD water and dried in air. Before electrodeposition of Cu-Ni film, the anodized Cu electrode was kept for 15 minutes in a solution mixture of 0.3 M $CuSO_4$, 0.3 M $NiSO_4$ and 0.5 M H_2SO_4 (5:5:2 v/v), which was referred to as precursor solution, for effective contacting with electrode surface. Then, a step potential of -6 V was applied for 70 s in a solution mixture of 0.3 M $CuSO_4$ and 0.3 M $NiSO_4$ (1:1 v/v). During the cathodic electrodeposition process, the porous Cu-Ni film was generated on the bare Cu electrode surface with the concurrent release of hydrogen bubbles acting as soft templates. In the next step, Cu-Ni film modified electrode was scanned by CV method in the potential range of -0.2 to 0.8 V in 0.1 M NaOH to convert Cu and Ni nanoparticles to the nano-scaled Cu_xO-NiO film. At the end of the synthesis procedure, Cu_xO-NiO modified Cu electrode was carefully rinsed with DD water, dried and kept in the air for further experiments. Eregress software was utilized to determine the optimum deposition conditions, including applied potential and its duration, as well as relative volume percent of 0.3 M $CuSO_4$ and 0.3 M $NiSO_4$ as model factors. The central composite design was used to prepare a model for obtaining optimized conditions.

Results and discussion

Characterization of nanostructured modified Cu electrode

A novelty of this work is related to a newly proposed method for preparing Cu-Ni nanocomposite film on the electrode surface, including a novel mixing method for modifier solutions. The method is

very fast, straightforward and cheap compared to other methods which have been previously used for fabricating composite materials, like fabrication of Cu-Ni by mechanically alloying [24] or some other techniques [25,26]. It must be stressed that here proposed method could also be applied in producing other electroactive composites for detecting other materials.

The surface examination of Cu$_x$O-NiO/Cu electrode under FESEM proved formation of nano-sized and non-uniform porous structures (Figure 1).
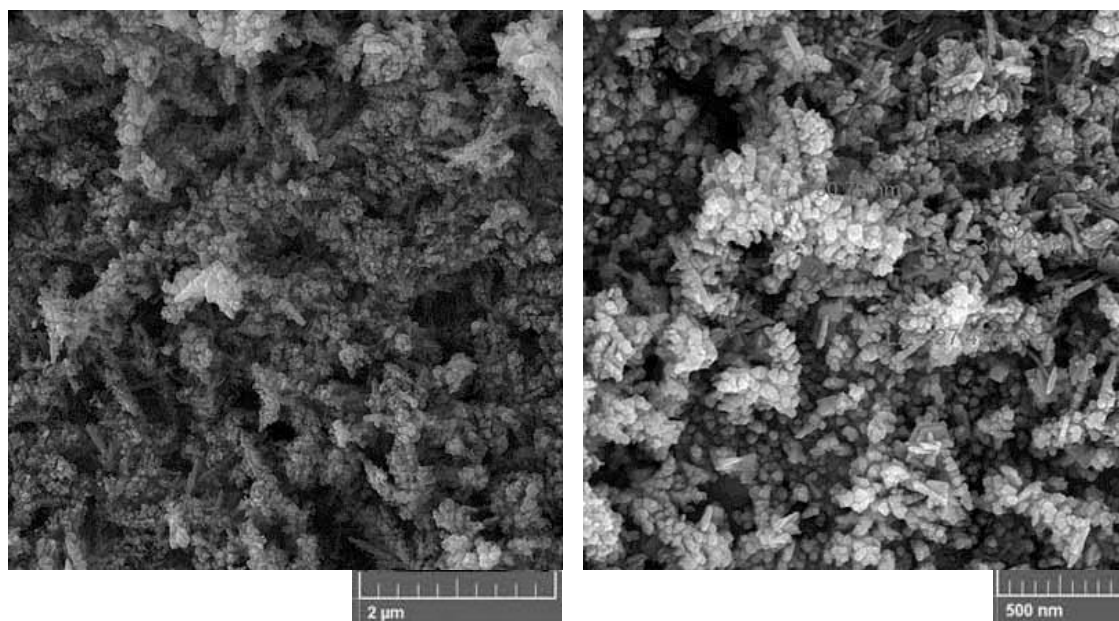

Figure 1. SEM images of Cu$_x$O-NiO film at different magnifications

The use of porous films with non-uniform pores resulted in better efficiency compared to traditional porous films [27]. Presence of nanoparticles deposited on Cu electrode is clearly demonstrated in Figure 1. The obvious porosity of the electrode surface is due to the hydrogen bubble evolution. By applying a high negative step potential for a limited time, a deposition of nano-scaled particles is generally expected because particles could not expand their size and participate in the nucleation process. In the present case, nanoparticles had just 70 s to deposit on the electrode surface at -6 V and therefore, they deposit along each other in a sloppy manner. The phase characteristics of the modified electrode are identified from its XRD pattern. As depicted in Figure 2 the diffraction peaks of the modified film are well indexed as monoclinic CuO (JCPDS no. 45-0937), Cu$_2$O (JCPDS no. 34-1354), NiO (JCPDS no. 47-1049), Cu (JCPDS no. 04-0836) and Ni (JCPDS no. 04-0850), respectively.
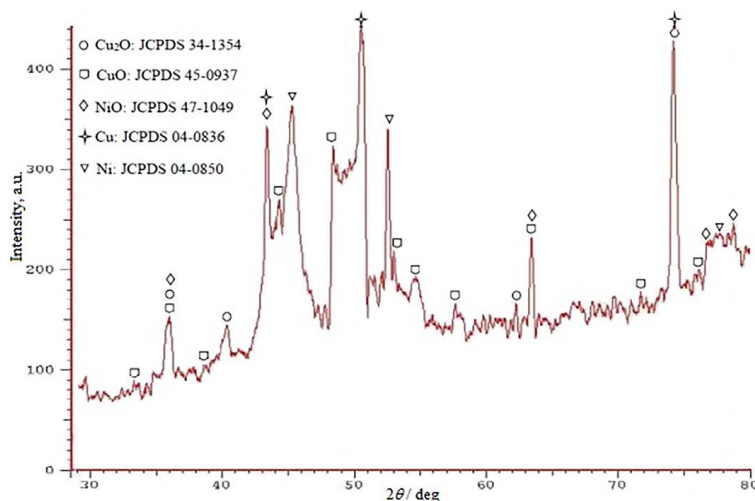

Figure 2. XRD pattern of Cu$_x$O-NiO film

Optimization of electrodeposition process by experimental design method

Central composite experimental design (CCD) was applied for simultaneous optimization of experimental parameters. CCD method is useful to determine the number of experiments that must be performed for the optimization of variables (factors) and responses. CCD uses the response surface methodology (RSM) to optimize experimental conditions. RSM is a widely used mathematical and statistical method for modeling and analyzing a process in which the response of interest is influenced by various variables and the goal of this method is to optimize the response. A key aim of experiment was to determine how significant each factor is. It is discussed how to design an experiment that allows sufficient degrees of freedom to determine the significance of a given factor. In the following section, the procedure of proving significance of each factor is explained. There are many situations, in which this information would be useful. After checking different parameters in CCD, one model is defined for obtaining the best conditions of synthesis, which get the response as a function of effective parameters. Multiple linear regression (MLR) method is used for modelling and the coefficients are calculated. The effect of three independent electrodeposition variables (E, t and v) on the system response is approximated by the second degree polynomial (MLR) equation:

$$\text{response} = b_0 + b_1E + b_2t + b_3v + b_4E^2 + b_5Et + b_6t^2 + b_7v^2 \tag{1}$$

According to eq. (1), the response for optimization of three factors, *i.e.* applied potential (E), applied potential duration (t) and relative volume percent (v), involves b_0 as an intercept or average, b_1E, b_2t and b_3v as linear terms depending on each of three factors, b_5Et interaction term between factor E and t, and also b_4E^2, b_6t^2, and b_7v^2 quadratic terms depending on each of three factors. Greater coefficients in eq. (1) show a more effective parameter and positive signs of coefficients describe that with their increasing, the response is increased as well. Some of the obtained characteristics of the designed model calculated by experimental design software (Eregress) are: $b_0 = -0.179$, $b_1 = -0.06307$, $b_2 = 0.00406$, $b_3 = 0.00642$, $b_4 = -0.00659$, $b_5 = -0.000217$, $b_6 = -3.92673 \times 10^{-5}$, $b_7 = -6.68436 \times 10^{-5}$. Since coefficients b_2 and b_3 have the highest values, t and v are defined as the most effective factors in the response.

In this work, Eregress software was used for interpreting the effect of both first and second order of parameters. The minimum, intermediate, and maximum values of each variable are labeled as −1, 0, and +1, respectively. If P-value (probability value) for each variable was greater than 0.05, it would not have significant effect in the model and takes zero value. If P-value was greater than 0.05 but the higher order of this factor had P-value less than 0.05, the variable was not removed.

Table 1 shows R^2 (coefficient of determination), that was improved by eliminating some unimportant variables ($P > 0.05$). R^2 is a statistical measure that shows the proportion of the variance for a dependent variable that is affected by all independent variables in a regression model. In other words, R^2 assumes that every independent variable explains the variation in the dependent variable.

***Table** 1. Coefficients of determination of prepared statistical model*

R^2	Adjusted R^2	Predicted R^2
0.946	0.908	0.747

The adjusted R^2, however, increases only if the new term improves the model more than would be expected by chance. Therefore, in statistical modeling, adjusted R^2 was also determined. The predictive power of the model has been proved by the predicted R^2 value. This parameter was obtained from the sum of squares of predicted errors. Comparing of R^2, adjusted R^2 and predicted R^2 can be a convenient technique to understand the conformity of a model. In a good model these

three parameters should not be too different. As shown in Table 1, R^2, adjusted R^2 and predicted R^2 have acceptable values for the model conformity.

For obtaining the optimum conditions of studied parameters, the surface response plots (plots show response as surfaces) were constructed. The optimum values can be derived using these plots. In these plots, all the minimum or maximum values of response for relative volume (*V* / %), *E* and *t* were investigated. Also, the relationship between the dependent and independent variables can be understood by these plots. Since the model has more than two factors, one factor was always kept constant. The example of surface response plot is shown in Figure 3. This figure demonstrates the interaction between relative volume (*v*) and *E* when *t* was kept constant. Response numbers show how much the factors influence another variable. Maximum response for each factor was selected according to surface response. As a general result, the optimized values for the applied potential, deposition time and relative volume percent were determined to be -6 V, 70 s and 50 % (1:1 v/v), respectively where the current or response was maximum in the corresponding surface response plots.
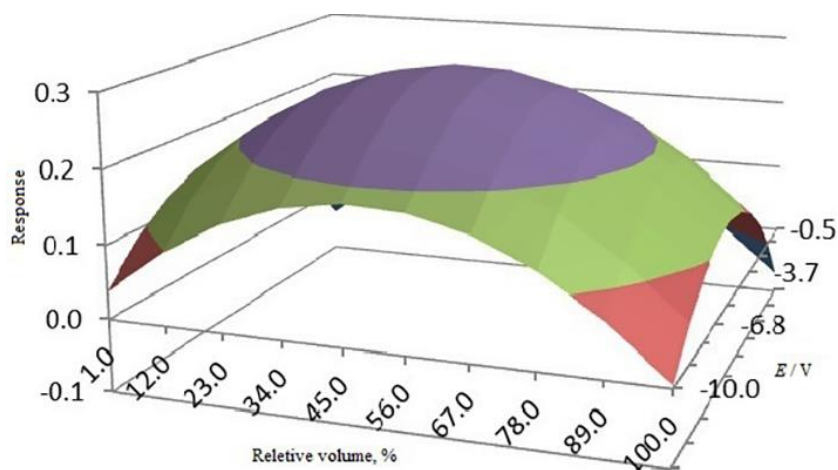

Figure 3. *Surface response representation related to RSM for optimizing two variables (E and relative volume, when* t *was kept constant).*

Cyclic voltammograms and electro-oxidation behavior of glucose at Cu$_x$O-NiO modified Cu electrode

Cyclic voltammograms in Figure 4 show that Cu (a), Ni (b) and Cu-Ni (c) particles can deposit separately or along each other at -6 V. However cyclic voltammogram for Cu$_x$O-NiO shows higher current of the overall redox process. Maybe the synergistic effect of Ni and Cu particles along each other is the reason for this phenomenon. It must be stressed here that according to our previous experiments performed under optimum conditions, presence of 0.3 M NiSO$_4$ in the deposition solution of 0.3 M CuSO$_4$ resulted in an increased current of the redox peaks in cyclic voltammograms and chronoamperograms.

Cyclic voltammograms in Figure 4 are in accordance with other studies [1,28]. It is seen in Figure 4a, that the modified Cu$_x$O electrode provides broad anodic and cathodic peaks attributed to successive Cu$^+$/Cu^{2+} and Cu^{2+}/Cu^{3+} redox pairs in the alkaline solution within the specified potential region [28]. Figure 4b shows Ni^{2+}/Ni^{3+} redox pair for NiO film, what is in well agreement with Ref. [14]. Therefore, Cu$^+$/Cu^{2+}, Cu^{2+}/Cu^{3+} and Ni^{2+}/Ni^{3+} redox pairs would play the main role in redox process of Cu$_x$O-NiO film modified electrode.

Figure 5 compares the electro-oxidation behaior of Cu$_x$O-NiO film electrode in alkaline medium with and without presence of glucose in the potential range of -0.2 to 0.8 V.
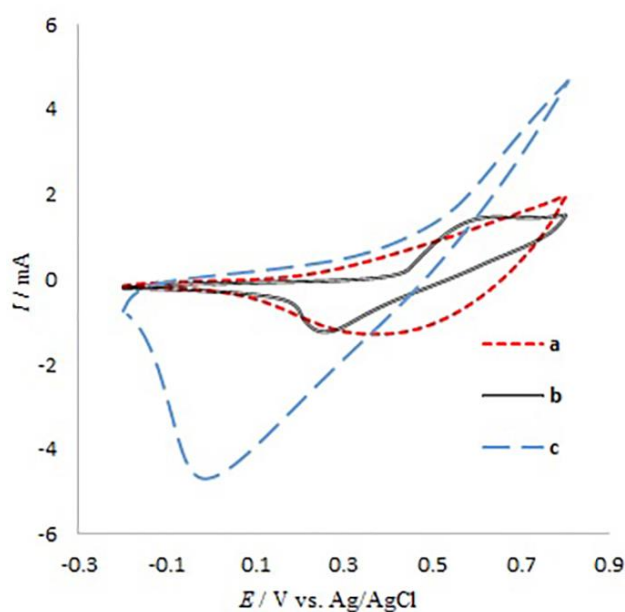
Figure 4. *Cyclic voltammograms of (a) CuₓO (b) NiO and (c) CuₓO-NiO film electrode in 0.1 M NaOH (v = 0.05 V/s)*

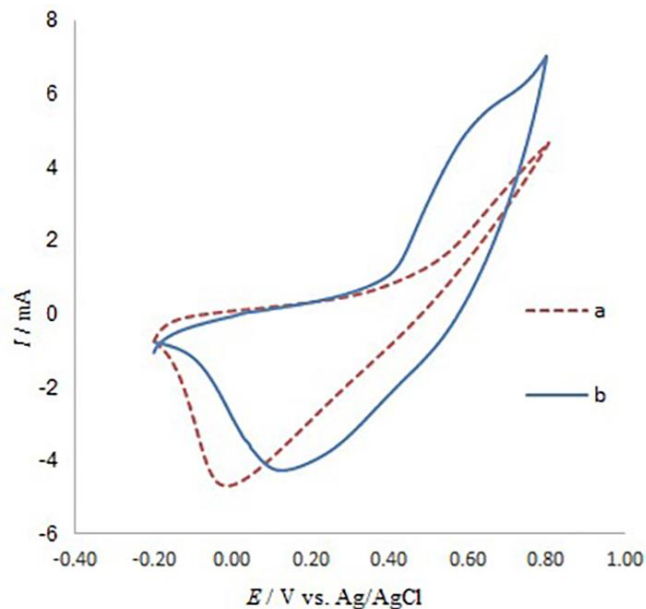**Figure 5.** *Comparison of the electro-oxidation behavior of CuₓO-NiO film electrode in 0.1 M NaOH in(a) absence and (b) presence of 2.87 mM glucose (v = 0.05 V/s)*

Oxidation of glucose started at about 0.45 V and caused an increase in current as observed. By adding only 2.87 mM glucose, a current difference of about 0.43 mA has been observed, what is observable on the current scale of mA and in accordance with chronoamperograms demonstrated below. The electrons resulting from the oxidation of glucose transfer directly to the electrode surface and result in the increase of anodic current at approximately 0.45 to 0.8 V during scanning. During the potential scan, the modified electrode surface can be oxidized, while the deprotonation of glucose molecules in an alkaline medium trigger isomerization to an enediol form, which then oxidizes to gluconolactone and then further hydrolyzes to gluconic acid [28].

Amperometric detection of glucose at CuₓO-NiO modified Cu electrode

Figure 6 illustrates chronoamperograms of 0.05 M glucose at different electrode modifying stages (before modifying, after anodizing and after electrodeposition), showing the effect of each modifying step.
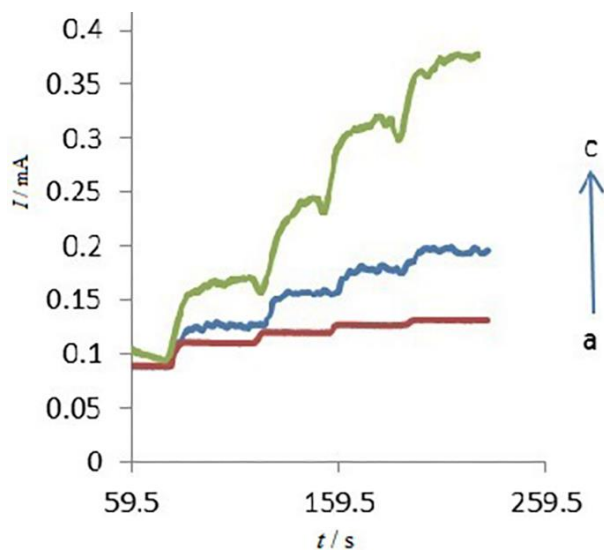

Figure 6. *CHA detection of 0.05 M glucose at (a) bare Cu electrode, (b) anodized Cu electrode, (c) anodized and cathodized Cu electrode*

According to Figure 6, the best chronoamperogram with the highest current response is obtained after fabricating Cu_xO-NiO modified Cu electrode. Finally, the fabricated non-enzymatic glucose sensor is applied for real samples such as human blood serum and urine at optimized condition using the CHA technique. The data of glucose evaluation in real samples obtained using the proposed sensor and data obtained from the local hospital were in full accordance.

The optimized step potential for chronoamperometric measurements of glucose was determined as 0.6 V. The chronoamperogram related to the addition of glucose into stirred 0.1 M NaOH solution is shown in Figure 7a. It is obvious that increase of the concentration of glucose in the electrolyte resulted in increase of the amperometric current value.
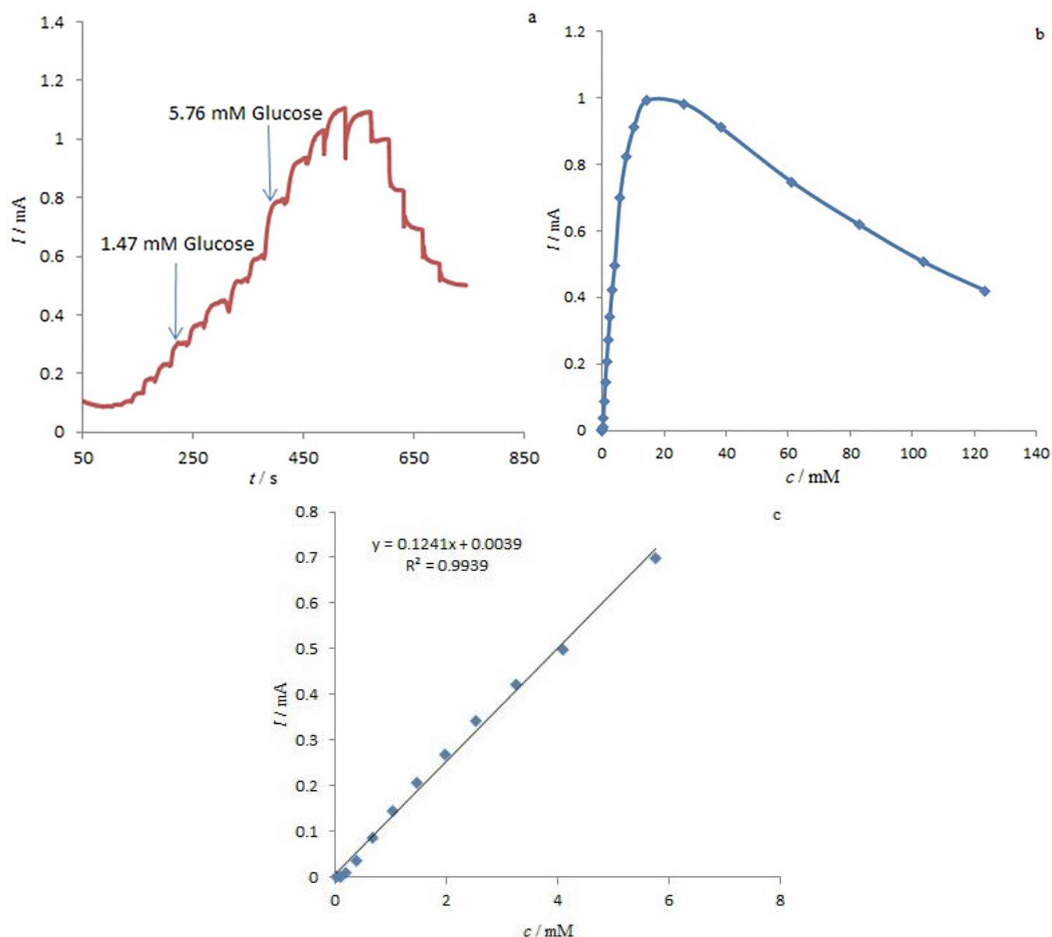

Figure 7. (a) CHA response of Cu_xO-NiO modified Cu electrode upon optimized conditions after successive additions of glucose into 0.1 M NaOH, (b) relationship between current and glucose concentration relevant to Figure 7a, and (c) the corresponding calibration curve for glucose.

The proposed sensor, however, lost its performance after the exposure to high concentrations of glucose, what is probably due to destruction of its active sites. Thus, the sensor shows decreased current values at high concentrations of glucose. Figure 7b demonstrates the relationship between currents and glucose concentrations, while Figure 7c shows the corresponding calibration plot for glucose concentration in a linear range from 0.04 to 5.76 mM.

Low limit of detection (LOD), equal to $0.0073 \pm 4.16 \times 10^{-4}$ mM and limit of quantification (LOQ) of $0.0243 \pm 1.38 \times 10^{-3}$ mM (signal/noise (S/N) = 3, n= 3 and confidence limit= 95 %) were determined. The calculated sensitivity of the proposed sensor was 1.38 mA mM^{-1} cm^{-2} which is signifycantly higher compared to data reported in previous studies for CoOOH nanosheets (0.34 mA mM^{-1} cm^{-2}) [29], or NiONPs/GO (1.09 mA mM^{-1} cm^{-2}) [30]. In this work, the obtained LOD of 7.3 µM is much better than

obtained for Cu_xO-Cu (49 µM) and gold nanotube array electrodes (10 µM) [7,31]. The calibration plot linearity range for our sensor is between 0.04 and 5.76 mM which is an order of magnitude higher than for CuO nanoleaves/MWCNTs (0–0.9 mM) [32].

Results obtained after comparison of the performance of fabricated glucose sensor with other enzyme less glucose sensors are shown in Table 2. It is seen in Table 2 that here proposed sensor is superior among most of other compared sensors, what is mainly due to its high sensitivity, low LOD and wide linear range.

Table 2. *Analytical data for glucose evaluation of the proposed Cu_xO-NiO/Cu nanosensor and other modified electrodes*

Working electrode	Linear range of concentration, mM	Sensitivity, mA mM^{-1} cm^{-2}	LOD, µM	Ref.[a]
Cu_xO-NiO/Cu	0.04–5.76	1.38	7.3	This Work
CuO nanoleaves/MWCNTs[b]	0–0.9	0.6643	5.7	[32]
Cu_xO/polypyrrole	0–0.8	0.232	6.2	[33]
NiO-Cu	0.01–2.14	4.02	1.7	[14]
Cu cubes/MWCNTs	0.5–7.5	0.922	2.0	[34]
Cu_xO	0–6	1.62	49	[7]
Platinum oxide layers	1–10	0.0056	800	[35]
SiO$_2$/C/CuO	0.02–20	0.472	0.06	[36]
ATCSNC[c] spheres	1–8.1	1.968	0.19	[37]
Pt@CNOs[d]	2–28	0.0216	90	[38]
Au/NiAu	0.005–31	0.483	1.0	[39]
Au@Cu$_2$O	0.05–2.0	0.715	18	[40]
Cu@Ni	0.001–4.1	0.78	0.5	[23]
CuNi-NGr[e]/GCE	Up to 20	7.143	10	[19]
Polyaniline/zinc oxide/ MWCNTs	0.1–1, 1–6	7.83, 1.67	0.0001	[41]

[a]Reference, [b]Multi-walled carbon nanotubes, [c]Ag@TiO$_2$ core-shell nano composite, [d]Carbon nano-onions, [e]CuNi-nitrogen doped graphene.

Selectivity and poison resistance of Cu_xO-NiO nanosensor

Selectivity against interfering species such as AA, UA and DA is crucial for a sensor. Amperometric currents recorded upon addition of glucose and these interfering species are depicted in Figure 8, showing the favorable selectivity of the proposed nanosensor for glucose monitoring. For most of the non-enzymatic glucose sensors based on precious metals and alloys, however, the activity can be easily lost due to the poisoning by chloride ions [9]. The amperometric current for Cu_xO-NiO modified electrode toward glucose detection, however, is found almost constant in 0.1 M NaOH in the presence and absence of 0.15 M NaCl. Therefore, the proposed sensor has demonstrated good poison-resistance ability towards chloride ions.
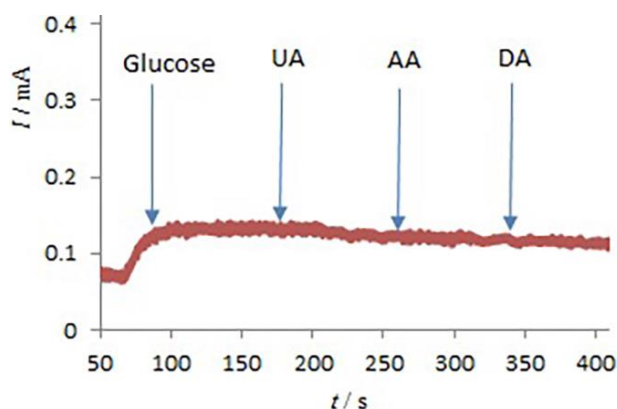

Figure 8. *CHA response of Cu_xO-NiO modified electrode upon addition of glucose, UA, AA and DA of equal concentrations (0.05 M) and equal volumes of 1 ml into 0.1 M NaOH upon optimized condition.*

Stability and reproducibility of Cu_xO-NiO nanosensor

Stability and reproducibility should be checked for any proposed sensor. In the present paper, stability of Cu_xO-NiO modified Cu electrode was monitored over the one month period. The sensor was kept in the refrigerator (4 °C) and evaluated each day for ten consecutive days and every five days over the next twenty days. After monitoring for one month, the sensor lost only 6.3 % of its efficiency in glucose detection. Moreover, we studied the reproducibility of the developed nanosensor by recording the amperometric current responses towards 0.6 mM glucose. Data of 7 parallel tests for each analyte showed a relative standard deviation RSD, % of $5.1 \pm 4.02 \times 10^{-3}$. Thus, the proposed non-enzymatic sensor showed favorable stability and reproducibility for glucose determination.

Conclusion

A new, simple, and low-cost electrochemical method is proposed for preparation of Cu_xO-NiO nanofilm on a bare Cu electrode for enzyme-free glucose sensing. The high electro-catalytic behavior could be attributed to the large electrochemical surface of the modified electrode, resulted from electrodeposition of nanostructured particles. Moreover, the fabricated sensor showed high sensitivity, a wide linear range, high stability (only 6.3 % decrease in performance in one-month time period), favorable precision and accuracy. The results from the determination of glucose concentration in blood serum and urine samples complied with those obtained from the local hospital. Thus, this easily fabricated Cu_xO-NiO nanosensor, could be applied as a practical sensor for routine analysis of glucose in clinical samples.

References

[1]   X. Niu, Y. Li, J. Tang, *Biosensors and Bioelectronics* **51** (2014) 22-28.
[2]   S. R. Lee, Y. T. Lee, K. Sawada, *Biosensors and Bioelectronics* **24** (2008) 410-414.
[3]   R. Wilson, A. P. F. Turner, *Biosensors and Bioelectronics* **7** (1992) 165-185.
[4]   M. Willander, L. L. Yang, A. Wadeasa, *Journal of Materials Chemistry* **19** (2009) 1006-1018.
[5]   S. Cosnier, R. E. Ionescu, M. Holzinger, *Journal of Materials Chemistry* **18** (2008) 5129-5133.
[6]   S. Park, H. Boo, T. D. Chung, *Analytica Chimica Acta* **556(1)** (2006) 46-57.
[7]   C. Li, Y. Su, S. Zhang, *Biosensors and Bioelectronics* **26** (2010) 903-907.
[8]   I. Kim, D. Kwon, D. Lee, T. H. Lee, J. H. Lee, G. Lee, D. S. Yoon, *Biosensors and Bioelectronics* **102** (2018) 617-623.
[9]   C. M. Welch, R. G. Compton, *Analytical and Bioanalytical Chemistry* **384(3)** (2006) 601-619.
[10] S. Park, T. D. Chung, H. C. Kim, *Analytical Chemistry* **75(13)** (2003) 3046-3049.
[11] J. S. Ye, Y. Wen, W. D. Zhang, *Electrochemistry Communications* **6(1)** (2004) 66-70.
[12] Y. Liu, H. Teng, H. Q. Hou, *Biosensors and Bioelectronics* **24** (2009) 3329-3334.
[13] H. Zhu, X. Lu, M. Li, *Talanta* **79(5)** (2009) 1446-1453.
[14] M. Hasanzadeh, R. E. Sabzi, *Current Chemistry Letters* **4** (2015) 45-54.
[15] Y. Zhang, Y. Wang, J. Jia, *Sensors and Actuators B: Chemical* **171–172** (2012) 580-587.
[16] F. Cao, S. Guo, H. Y. Ma, *Biosensors and Bioelectronics* **26** (2011) 2756-2760.
[17] C. C. Li, Y. L. Liu, L. M. Li, *Talanta* **77(1)** (2008) 455-459.
[18] L. Zhang, Y. H. Ni, H. Li, *Microchimica Acta* **171** (2010) 103-108.
[19] L. Shabnam, S. N. Faisal, A. K. Roy, A. I. Minett, V. G. Gomes, *Electrochimica Acta* **224** (2017) 295-305.
[20] L. Nei, *Journal of Analytical Chemistry* **367** (2000) 436-439.
[21] Y. He, G. Wei, J. Lin, M. Sun, *Electroanalysis* **29(4)** (2017) 965-974.
[22] D. Wang, B. Huang, J. Liu, X. Guo, G. Abudukeyoumu, Y. Zhang, B. C. Ye, Y. Li, *Biosensors and Bioelectronics* **102** (2018) 389-395.

[23]   K. L. Wu, Y. M. Cai, B. B. Jiang, W. C. Cheong, X. W. Wei, W. Wang, N. Yu, *RSC Advances* **7** (2017) 21128-21135.
[24]   I. S. Ahn, T. H. Nam, S. R. Bae, *Metals and Materials International* **3(4)** (1997) 260-264.
[25]   N. Karthik, T. N. J. I. Edison, M. G. Sethuraman, Y. R. Lee, *Applied Surface Science* **396** (2017) 1245-1250.
[26]   P. E. Sharel, D. Liu, R. A. Lazenby, J. Sloan, M. Vidotti, P. R. Unwin, J. V. Macpherson, *The Journal of Physical Chemistry C* **120(29)** (2016) 16059-16068.
[27]   S. Cherevko, C. H. Chung, *Talanta* **80(3)** (2010) 1371-1377.
[28]   S. K. Meher, G. R. Rao, *Nanoscale* **5** (2013) 2089-2099.
[29]   K. K. Lee, P. Y. Loh, C. H. Sow, *Electrochemistry Communications* **20** (2012) 128-132.
[30]   A. Salimi, A. Noorbakhash, E. Sharifi, *Biosensors and Bioelectronics* **24** (2008) 792-798.
[31]   Y. G. Zhou, S. Yang, Q. Y. Qian, *Electrochemistry Communications* **11(1)** (2009) 216-219.
[32]   Z. Y. Yang, J. S. Feng, J. S. Qiao, *Analytical Methods* **4** (2012) 1924-1926.
[33]   F. H. Meng, W. Shi, Y. N. Sun, *Biosensors and Bioelectronics* **42** (2013) 141-147.
[34]   J. Zhao, L. M. Wei, C. H.Peng, *Biosensors and Bioelectronics* **47** (2013) 86-91.
[35]   A. Weremfo, S. T. C. Fong, A. Khan, D. B. Hibbert, C. Zhao, *Electrochimica Acta* **231** (2017) 20-26.
[36]   A. Rahim, Z. U. Rehman, S. Mir, N. Muhammad, F. Rehman, M. H. Nawaz, M. Yaqub, S. A. Siddiqi, A. A. Chaudhry, *Journal of Molecular Liquids* **248** (2017) 425-431.
[37]   T. Dayakar, R. K. Venkateswara, M. Vinodkumar, K. Bikshalu, B. Chakradhar, R. K. Ramachandra, *Applied Surface Science* **435** (2018) 216-224.
[38]   J. Mohapatra, B. Ananthoju, V. Nair, A. Mitra, D. Bahadur, N. V. Medhekar, M. Aslam, *Applied Surface Science* **442** (2018) 332-341.
[39]   L. Wang, W. Zhu, W. Lu, X. Qin, X. Xu, *Biosensors and Bioelectronics* **111** (*2018)* 41-46.
[40]   Y. Su, H. Guo, Z. Wang, Y. Long, W. Li, Y. Tu, *Sensors and Actuators B: Chemical* **255** (2018) 2510-2519.
[41]   S. Mohajeri, A. Dolati, K. Yazdanbakhsh, *Journal of Electrochemical Science and Engineering* **9(2)** (2019) 207-222.